Eur Biophys J (2005) 34: 170–179
DOI 10.1007/s00249-004-0440-1

ARTICLE

Bruno Demé · Damien Marchal

Polymer-cushioned lipid bilayers in porous alumina

Received: 2 June 2004 / Revised: 16 September 2004 / Accepted: 21 September 2004 / Published online: 5 November 2004

Abstract Using small-angle neutron scattering (SANS) and cyclic voltammetry (CV), we show that model biological membranes can be deposited on a polymer cushion confined in highly regular porous alumina. The thicknesses of the dilute polymer cushion chemically bound to the alumina and of the supported bilayer are obtained for two polyethylene glycol cushions (PEG_{5000} and PEG_{20000}) and for a cushion made of chains bearing a lipid anchor at their free end (DSPE-PEG_{3400}). The bilayers are studied well below and well above the chain melting temperature of the lipid mixture (DMPC/DMPE: 80/20), using a coenzyme (Ubiquinone, UQ_{10}) as a redox probe for the voltammetry experiments. Analysis of the SANS form factor of the bilayers shows that the bilayer thickness can be extracted in this particular geometry. Using PEG chains grafted at a low surface density ($D < 2R_g$), the thickness of the complete molecular construction is obtained by CV, which shows (after subtracting the bilayer thickness) that the polymer cushion thickness can be varied from 50 to 150 Å. The values obtained with three different chain lengths, are in perfect agreement with the radius derived from the Flory theory.

Keywords Solid-supported membranes · PEG · Ubiquinone · SANS · Electrochemistry · Diffusion

Introduction

A variety of biological processes that occur in biological membranes require a fluid lipid bilayer that enables lateral diffusion of membrane components and translocation processes. This essential condition must be fulfilled in both free and solid-supported membrane models. In the case of solid-supported membranes, it is therefore preferable to separate the lipid bilayer from the underlying surface, so that an aqueous compartment between the solid support and the bilayer is formed (Sackmann 1996). This can be achieved by several means; see for example Charitat et al. (1999) for lipid bilayers floating on top of a first lipid layer bound to a silicon wafer, or Seitz et al. (1998) for a polymer-cushioned bilayer covering the surface of a glass slide. In this case, depending on the grafting density of the chains on the solid support, one can distinguish dense cushions made of entangled polymer chains grafted at a density such that the polymer chains interact—the brush regime—from chains in the dilute regime separated by a distance (D) larger than twice their radius of gyration ($2R_g$)—the so-called mushroom regime. A dilute polymer layer is sufficient to tether lipid structures (Spinke et al. 1992; Heyse et al. 1998; Seitz et al. 1998; Wagner and Tamm 2000; Knoll et al. 2000). It restores the aqueous phase missing in most solid-supported membrane models and minimizes the interaction between the polymer and the bilayer (Naumann et al. 2002; Schmitt et al. 2001), and the thickness of the aqueous subcompartment is controlled by the lengths of the polymer chains.

Using a dilute polymer layer of polyethylene glycol chains offers another advantage when the formation of the bilayer is obtained by spontaneous fusion of vesicles onto the surface. PEG chains are known to promote fusion of lipid vesicles (Proux-Delrouyre et al. 2001; Lipowsky and Sackmann 1996). Therefore, using a dilute layer of PEG chains is a way of promoting fusion of lipid vesicles without resorting to lipid anchors bound to the chains like thio-lipids (Lang et al. 1994), thio-peptide-lipids (Bunjes et al. 1997), biotin-lipids (Proux-Delrouyre et al. 2001) or metal-chelator-lipids (Rädler et al. 2000).

The model of a biological membrane presented in this paper (Fig. 1) is derived from a previous study (Marchal et al. 1998). Above the chain melting transition, it is a fluid floating bilayer, separated from its solid support by

B. Demé (✉)
Institut Laue-Langevin, BP 156, 38042 Grenoble Cedex 9, France
E-mail: deme@ill.fr

D. Marchal
Laboratoire d'Electrochimie Moléculaire—UMR 7591,
Université Paris 7 Denis Diderot, CNRS,
75251 Paris Cedex 05, France
E-mail: marchal@paris7.jussieu.fr

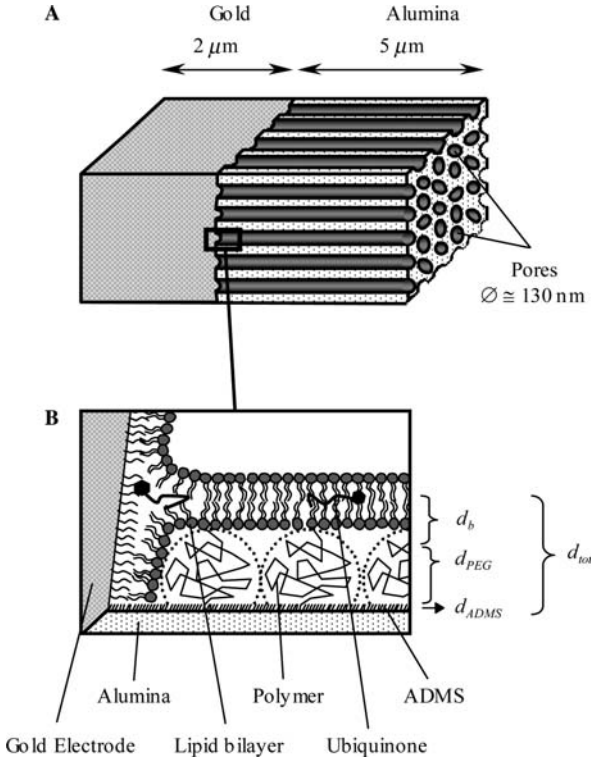

Fig. 1 **a** Structure of the microporous electrode made of porous aluminum oxide film attached to a gold electrode. The porous oxide is the host of the self-assembled lipid bilayer. For a 3 mm diameter electrode, the effective surface area is ~5 cm^2. **b** Enlarged schematic view of the bottom of a pore at the level of the polymer-supported bilayer/gold interface. UQ_{10} molecules are laterally mobile along the pore wall and reach the electrode at this level. d_{ADMS}, d_{PEG}, d_b and d_{tot} represent the thicknesses of the ADMS layer, the polymer layer, the bilayer, and the sum of the ADMS, PEG and bilayer thicknesses, respectively

an aqueous sub-compartment whose thickness is controlled at the molecular scale. The approach is based on the use of the original geometry provided by the microporous alumina used in the microporous electrode employed in electrochemical studies of redox membrane proteins (Marchal et al. 2001b). Thanks to the insulating properties of alumina, and to the possibility of deriving the alumina into a gold electrode, the host—the bilayer bound to its solid support—is perfectly suited to electrochemical studies of redox membrane enzymes.

This study describes our efforts to develop a host for integral and peripheral redox membrane proteins, suited both to structural studies by scattering techniques and to electrochemical studies of the enzymes' activity in their native state.

We therefore combined small-angle neutron scattering (SANS) on these model membranes (the enzyme host) aligned by the solid support (the membrane host) with the methodology developed for electrochemical studies of redox enzymes (Marchal et al. 2001a). Combining SANS with voltammetry is an alternative to other surface techniques not suited to studies of bilayers confined in an opaque, porous but highly oriented and extremely smooth surface at molecular scale. Electrochemistry is well suited to the study of heterogeneous media like biological membranes. The electrochemical detection of a redox probe confined in a lipid bilayer leads to information on the state of the bilayer, fluid or frozen, and to its viscosity (Marchal et al. 1998). Combined with the geometry of a porous environment, electrochemistry is also a technique which allows the detection of a water-soluble redox probe and determination of the decrease in pore size due to the presence of structures bound to the pore wall (Proux-Delrouyre et al. 2002). SANS is the technique of choice for the study of these layered interfacial structures of increasing complexity at each step of the self-assembly. It offers a unique ability to contrast-match alumina in a H_2O/D_2O mixture, the relatively high scattering length density of which yields an excellent contrast with protonated biological materials. It also results in a low incoherent background due to the relatively low incoherent scattering cross-section of the samples. Alumina (Al_2O_3), which represents about 50% of the sample volume, contributes very weakly to the incoherent background due to the low incoherent scattering cross-section of aluminum and to the zero cross-section of oxygen. Therefore, in this work we focused on scattering by the interfacial layers in pure D_2O. Our previous study on hybrid OTS-DMPC bilayers (Marchal et al. 2001a) indicated that working in pure D_2O yields an even better contrast, although the solid support is no longer matched to the solvent. Removing any trace of H_2O further reduces the incoherent signal and makes it possible to measure $I(q)$ down to very low intensities. Furthermore, the potential of the SANS technique is increased by the use of a regular 2-D hexagonal matrix of cylindrical pores oriented in a coaxial geometry relative to the neutron beam. In this configuration, the incident neutron beam is parallel to the pore long axis and therefore to the membrane plane. This scattering geometry increases the intensity by more than one order of magnitude compared to an equivalent but randomly oriented interface (Marchal and Demé 2003).

The cyclic voltametry (CV) experiments are performed with two different probes: the hydrophobic ubiquinone (UQ_{10}, the natural coenzyme of the electron transfer chain in biological membranes), and a water soluble redox probe (ruthenium(III) hexamine). Combined with the SANS experiments, the results obtained with these two probes show the presence of a continuous and homogeneous bilayer at macroscopic scale (5 cm^2). They also lead to the thickness of both the bilayer and the aqueous polymer layer. Finally, we compare the thickness of the polymer layer to its unperturbed theoretical value (in the absence of the bilayer).

Experimental section

Reagents

The aluminum foils, 1 mm thick (Al 99.95%), were from Merck (Darmstadt, Germany). Aminopropyl-dimethylethoxysilane (ADMS), octadecyl mercaptan (OM) and

ruthenium(III) hexamine chloride were from Aldrich (Saint Louis, MO, USA). Methoxy-[poly-ethylene-glycol]$_n$-succinimidyl propionate (mPEG$_{5000}$-MPA and mPEG$_{20000}$-MPA) and 1,2-distearoyl-*sn*-glycero-3-phosphoethanolamine-[poly-ethylene-glycol]$_{3400}$-*N*-hydroxy-succinimidyl carbonate (DSPE-PEG$_{3400}$-NHS) were from Shearwater (Huntsville, AL, USA). 1,2-Dimyristoyl-*sn*-glycero-3-phosphocholine (DMPC, purity > 99%), 1,2-dimyristoyl-*sn*-glycero-3-phosphoethanolamine (DMPE, purity > 99%) were from Avanti Polar Lipids (Alabaster, AL, USA). Ubiquinone (UQ_{10}) and *n*-octyl *β*-D-glucopyranoside (OG) were from Sigma (Saint Louis, MO, USA). Organic solvents were HPLC grade. Water with a resistivity of 18 MΩ was produced by the Milli-Q purification system from Millipore (Billerica, MA, USA).

Preparation of microporous electrodes

Modified electrodes were produced in our laboratory according to the procedure first described by Miller and Majda (1985) and modified by Marchal et al. (1998). In the present work, the alkylation step was substituted for the formation of the ADMS and PEG layers. After separation of the aluminum oxide layer from the aluminum substrate, geometrical characterization of the alumina foil was performed by environmental scanning electron microscopy (ESEM XL 30 from Philips). Values found were: 5 ± 0.5 μm for the thickness, 3.5×10^{9} cm^{-2} for the pore density, and 130 ± 30 nm for the average pore diameter.

Preparation of the cushioned bilayers

The tethered bilayer is formed in three steps. The first step is to chemically graft the amino-silane (ADMS) to the aluminum oxide. This produces a homogenous layer with a high surface density of reactive groups (Moon et al. 1997). Amino groups were created at the surface of the aluminum oxide by reaction with a freshly prepared ADMS solution in toluene (2%, v/v) for 8 h, followed by rinsing extensively with toluene and drying.

The second step consists in grafting NHS-PEG chains to the amine group of the amino-silane layer. The derivatized oxides were immersed at ambient temperature in a 20×10^{-3} mol l^{-1} solution of mPEG$_{20000}$-MPA, mPEG$_{5000}$-MPA or DSPE-PEG$_{3400}$-NHS in dimethylformamide (DMF). The PEG-oxides were removed from the solvent after 12 h and were intensively rinsed with DMF, ethanol and dried.

The third step is the fusion of vesicles onto the polymer layer by direct contact between the PEG layer and vesicles. Mixed phospholipid-UQ_{10} vesicles were obtained from the dry lipid mixture as follows: the chloroform solution of DMPC, DMPE and UQ_{10} (78/20/2), was evaporated under nitrogen flow and dried under high vacuum for 1 h. The film was suspended from the walls of a glass tube by vigorous vortexing in 5 ml of buffer. The solution was sonicated until clarity was obtained, typically 4×3 min, with a Branson 250 sonicator (Danbury, CT, USA) at a power of 60 W, the temperature being maintained between 50 and 60 °C using a bath to avoid overheating and to keep the temperature of the vesicles above the chain melting transition temperature. A dispersion of small unilamellar vesicles (SUV, 1×10^{-3} mol l^{-1}) was used during the day. Fusion of unilamellar vesicles into the microporous electrode was realized by incubation of the electrode in the SUV solution at 40 °C for 30 min. Before use, the oxides were rinsed with water.

Confined in a porous volume, no direct information on the layer density can be obtained. However, the upper limit on the density of PEG chains obtained by self-assembling is lower than the density required for the chains to adopt a brush conformation (Anne et al. 2002). The maximum grafting density of PEG chains from a solution depends on the radius of gyration of the chains in solution and therefore on their length (de Gennes 1980). For solutions of PEG$_{3400}$, PEG$_{5000}$ and PEG$_{20000}$ at 20×10^{-3} mol l^{-1} these maximum grafting densities are 2.6×10^{-8}, 2.0×10^{-8}, and 1.6×10^{-8} g cm^{-2}, respectively. At such densities, the layer is highly hydrated and the chains are at the limit of the transition between isolated mushrooms and brushes. The low density PEG layers are then used in the third step as a promoting element for the fusion of the vesicles (Rajarathman et al. 1989; Lipowsky and Sackmann 1996).

Electrochemical measurements

The anaerobic electrochemistry cell contains three electrodes: the working microporous electrode, a platinum foil auxiliary electrode, and a KCl saturated aqueous calomel reference electrode (SCE = 0.234 V vs. the normal hydrogen electrode at 30 °C) to which all potentials are referred. Gentle bubbling of nitrogen reduced the partial pressure of oxygen in the main compartment. The temperature was controlled from 10 to 50 °C by water circulation in the outer compartment of the water-jacketed cell. For the rotating disk electrode (RDE) experiments, the microporous electrodes were introduced into a special holder at the tip of the rotating device (motor and speed control unit CTV101T from Tacussel Radiometer Analytical, Villeurbanne, France). The instrument for CV and RDE amperometry was a in-house-built potentiostat controlled by a PC.

Small-angle neutron scattering experiments

Neutron scattering experiments were performed on the D22 SANS instrument and on the D16 diffractometer at the high-flux reactor of the Institut Laue-Langevin, Grenoble, France. Unlike our preceding studies (Marchal et al. 2001a; Marchal and Demé 2003), we used only

two different settings on D22, covering a q-range of 3×10^{-3} to 6×10^{-1} Å^{-1}. The D16 q-range was 5×10^{-2} to 6×10^{-1} Å^{-1}.

Using only two settings instead of three on D22 results in a q_{min} higher than in our previous studies on pure alumina and hybrid bilayers (7×10^{-4} Å^{-1}). However, it remains sufficient to cover the bilayer form factor on which we concentrate here. It also means that the alumina structure factor cannot be seen anymore. The first Bragg reflection of the 2-D hexagonal structure factor of the pores is outside the q-range. The weak and broad second and third orders observed at $\sqrt{3}$ and $\sqrt{4}$ are covered by the q-range used in this work but the resolution of the configuration used to reach 3×10^{-3} Å^{-1} is much lower than the one used to reach 7×10^{-4} Å^{-1}, so they are simply smoothed out.

On both instruments, 60 μm-thick alumina sheets were held fully hydrated between circular quartz windows (1 mm thick quartz QS from Hellma) and oriented in the beam as described previously (Marchal et al. 2001a). We used commercial Anodisc filtration membranes instead of those produced in our laboratory whose thickness (5 ± 0.5 μm) is too low for SANS experiments. Both are produced by anodization and can be used in the microporous electrode. Compared to our 5 μm-thick membranes, Anodisc membranes (60 μm) represent an increase in the amount of interface in the beam by a factor of 12. The samples were measured in coaxial geometry: with the pore long axis parallel to the incident neutron beam. The alignment is performed by rocking the samples successively around the vertical and horizontal axis by means of a rotation table and a goniometer (precision of 0.01°), respectively.

Since the coaxial geometry leads to circular symmetry, perfectly isotropic 2-D patterns are obtained and 2-D raw data can be reduced to 1-D by radial averaging. The data were normalised to the monitor, and to the transmission and the thickness of the sample. The scattering by the quartz windows holding the sample and the instrument background were subtracted and water calibration runs were used to account for the detector efficiency and to normalise the data to the incoherent scattering cross-section of water. Finally, a flat background was subtracted to account for the incoherent scattering of the sample.

Analysis of small-angle neutron scattering data

The analytical relations describing the scattering (form and structure factors) by parallel cylinders in close packing and coaxial orientations (pore long axis parallel to the incident beam) are described elsewhere (Marchal and Demé 2003). See also Marchal et al. 2001a, b and references therein for hybrid bilayers chemically bound to the alumina surface.

Because of the dimensions of the cylinder, and in spite of their close packing, the alumina structure factor is only observed in the very low-q range, well below the range where the interface structure is observed. Therefore, according to the porous structure of alumina, our approach consists of considering the scattering produced by the interface only in the corresponding q-range. According to the pore diameter and center-to-center distance it has been shown that far from the very low q range, the intensity at wide q is dominated by the interface contribution. This approach was used in a previous study to characterize the surface of porous alumina membranes in the presence of a hybrid bilayer chemically bound to the alumina surface (Marchal et al. 2001a).

Considering the analytical relations describing the scattering by the bilayer, two distinct cases must be distinguished depending on whether the bilayer is directly in contact with the solid support (chemically bound or adsorbed) or separated by an aqueous layer.

In the former case (hybrid bilayer chemically bound to the alumina surface) the layer was directly in contact with the solid support, and the form factor is then given by (Marchal et al. 2001):

$$I(q) = \left[2\pi\Sigma\left(\Delta\rho_{1,3}\right)^2\frac{1}{q^4} + 2\pi\Sigma\left(\Delta\rho_{2,3}\right)^2\frac{1}{q^4}\left(1-\cos qd_b\right) - 4\pi\Sigma\left(\Delta\rho_{1,3}\right)\left(\Delta\rho_{2,3}\right)\frac{1}{q^4}\left(1-\cos qd_b\right)\right]e^{-\sigma^2q^2} \quad (1)$$

where Σ is the specific area of the porous material, $\Delta\rho$ the scattering length density contrast and d_b the bilayer thickness. The Porod term (Porod 1951) refers to the scattering by the alumina, the second term corresponds to the bilayer scattering, and the third one is the cross term (Marchal et al. 2001a). Indices in the contrast terms refer to the alumina (1), the bilayer (2), and the solvent (3). With a layer of constant thickness chemically bound to the solid support, the roughness and the specific area are the same for all interfaces, so that a single specific area (Σ) and a single roughness (σ) are sufficient to describe the system.

In the case of a layer separated from the solid support by an aqueous compartment, the analytical description simplifies to the sum of the Porod (1951) term and the bilayer form factor. The cross term disappears and Eq. 9 simplifies to:

$$I(q) = 2\pi\Sigma_1\left(\Delta\rho_{1,3}\right)^2\frac{1}{q^4}e^{-\sigma_1^2q^2} + 2\pi\Sigma_2\left(\Delta\rho_{2,3}\right)^2\frac{1}{q^4}\left(1-\cos qd_b\right)e^{-\sigma_2^2q^2} \quad (2)$$

However, since the bilayer is no more tightly bound to the solid support, we need to introduce a second specific area and a second roughness term. Here, σ_1 and σ_2 refer to the roughness of the solid support and of the bilayer, respectively. Then, since the floating bilayer is no more bound to the solid support, one may wonder whether the specific areas of the alumina and of the bilayer are still the same. If this is the case, another simplification of the model leads to:

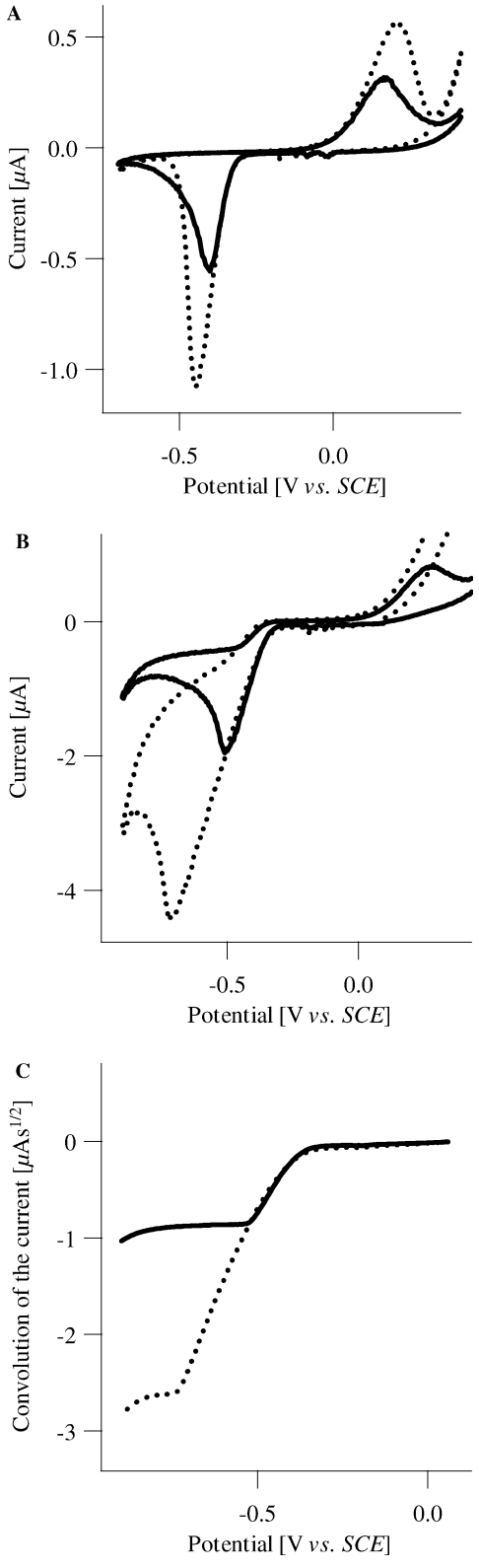

Fig. 2 Cyclic voltammograms obtained with a DMPC/DMPE/UQ_{10} (78/20/2) bilayer supported in the microporous electrode on a DSPE-PEG_{3400} cushion. **a** Low scan rate (0.01 V s^{-1}) at 27 °C (*solid line*) and 44 °C (*dashed line*). The concentration of UQ_{10} in the bilayer is determined from the peak area: 10×10^{-12} mol cm^{-2} at 44 °C, and 7×10^{-12} mol cm^{-2} at 27 °C. **b** fast scan rate (0.2 V s^{-1}) at 27 °C (*solid line*) and 44 °C (*dashed line*). **c** Cyclic voltammograms at fast scan rate from Fig. 2b are transformed by convolution of the current into a S-shaped curve: *solid line* for 27 °C and *dashed line* for 44 °C

Whether the bilayer is covering the entire porous surface or not, one should use a single value for Σ (Eq. 2), or two different values (Eq. 3). The answer to this point will be given by the voltammetry experiments and we shall come back to this point in the "Results" section.

$$I(q) = 2\pi\Sigma\left[\left(\Delta\rho_{1,3}\right)^2\frac{1}{q^4}e^{-\sigma_1^2q^2} + \left(\Delta\rho_{2,3}\right)^2\frac{1}{q^4}\left(1-\cos qd_b\right)e^{-\sigma_2^2q^2}\right] \quad (3)$$

Results

Continuity and homogeneity of the bilayer

UQ_{10} is strictly water insoluble. At sufficiently low UQ_{10} concentrations (below a UQ_{10}-to-lipid ratio of 2 mol%) UQ_{10} lies and moves only in the mid-plane of the bilayers (Marchal et al. 1998). The UQ_{10}/lipid ratio is unchanged after fusion of the vesicles to the surface (polymer-cushioned bilayer) (Marchal et al. 1998; Proux-Delrouyre et al. 2001). CV at low scanning rate (Fig. 2a, dashed line), corresponds to a large timescale that ensures that all active redox molecules can reach the electrode by lateral diffusion in the bilayer mid-plane. Integration of the current peak leads to the total amount of UQ_{10} confined in the supported bilayer. We derived a charge of 9.6 ± 0.3 μC. From the geometric area of the microporous structure (5 cm^2), the UQ_{10}-to-lipid ratio (2 mol%), and the mean area per lipid molecule in the bilayer (67 $Å^2$ for DMPC and 63 $Å^2$ for DMPE) (Rand and Parsegian 1989), the calculated UQ_{10} charge was found to be similar to the experimental results. This yields a UQ_{10} surface concentration of 9.4×10^{-12} mol cm^{-2}. The excellent agreement with the experimentally-derived charge demonstrates that the lipid bilayer bound to the polymer cushion covers the entire surface of alumina. Control experiments (not shown) also demonstrate that the final UQ_{10} charge is, as expected, proportional to the UQ_{10}-to-lipid ratio in the vesicles (in the range 1–3%). From these results one can conclude that there is no loss of UQ_{10} during and after the self-assembling process and that the entire porous surface of alumina is covered by the cushioned-bilayer. This is an important prerequisite to the SANS experiments for the choice of the analytical model to be used. We can already assume that the specific area of alumina and that of the bilayer (Σ_1 and Σ_2 in Eq. 2) are the same, so that Eq.3 can be applied to our system. We can also conclude from these results that the bilayer is defect-free along the pore walls (in the bilayer plane).

Fluidity of the two bilayer sub-foils

The micro-viscosity in the membrane core is directly related to the physical state of the lipid chains, liquid (L_α) or crystalline ($P_{\beta'}$, $L_{\beta'}$). As shown previously (Marchal et al. 1998), the lateral diffusion of UQ_{10} is described by the continuum fluid hydrodynamic model (Saffman and Delbrück 1975). Therefore, the diffusion of UQ_{10} localized in the mid-plane depends directly on the micro-viscosity in the bilayer according to:

$$D = \frac{kT}{16a\eta_{\text{bilayer}}} \tag{4}$$

where D is the lateral diffusion coefficient of UQ_{10}, k is the Boltzmann constant, T the temperature, a the radius of a flat cylinder representing UQ_{10} and η_{bilayer} the micro-viscosity in the bilayer core.

The determination of the diffusion coefficient of UQ_{10} is made possible by means of CV at a fast scanning rate. In these conditions, the measurement can be assimilated to a CV in an infinite medium because it corresponds to a timescale that ensures that the diffusion layer is thinner than the oxide film. In Fig. 2b, the thin solid line shows cyclic voltammograms of UQ_{10} in the polymer-cushioned bilayer at a fast scan rate, at 27 and 44 °C. Some distortion of the signal is observed, probably due to an uncompensated ohmic drop. This can be explained by the confinement of the electrical contact area between the partially blocked electrode, the bilayer and the solution. Therefore, the diffusion coefficient cannot be extracted directly from the experimental voltammograms with good precision. A transformation of the voltammogram into a S-shaped curve by convolution of the current with the time function $1/\sqrt{\pi\ t}$ is required. This function characterizes the linear diffusion (Andrieux and Savéant 1970). Figure 2c shows the cyclic voltammograms transformed into S-shaped curves. One of the advantages of the convolution method over the classical treatment of cyclic voltammograms is that the current plateau is independent from the ohmic drop and from the rate law of the electron transfer. It only depends on the diffusion coefficient:

$$Ip = \frac{Q_f\sqrt{D}}{2d} \tag{5}$$

where Q_f is the amount of UQ_{10} confined in the bilayer and d the length of the alumina pore (5 μm).

At 35 °C, D is found to be $4 \pm 1\times10^{-8}$ cm^2 s^{-1}, in good agreement with FRAP results (Rajarathnam et al. 1989; Chazotte et al. 1991) and previous chronocoulometry measurements (Marchal et al. 1998; Proux-Delrouyre et al. 2001).

Values for the micro-viscosities have been calculated from the experimental diffusion coefficient of UQ_{10} and using Eq. 5. Figure 3 shows the temperature dependence of the micro-viscosity in the bilayer in the form of an Arrhenius plot. One can see that the viscosity follows two regimes below and above 34 °C. Above 34 °C,

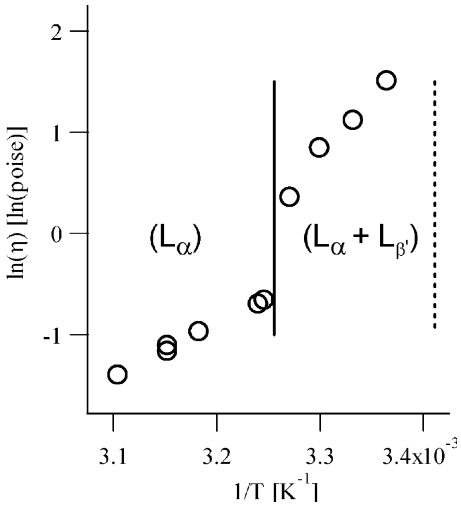

Fig. 3 Variation of the bilayer viscosity as a function of temperature. The viscosity is determined from the lateral diffusion coefficient of UQ_{10} according to Eq. 4. The *solid line* represents the limit between the (L_α) and the (L_α + $L_{\beta'}$) mixed phase and the *dashed line* the limit between the (L_α + $L_{\beta'}$) mixed phase and the ($L_{\beta'}$) phase for a DMPC/DMPE ratio of 80/20 (Silvius 1986)

apparent activation energies for the viscous flow (E_{visc}) are given by the slope of the linear fit to the data. The value of E_{visc} is 10 ± 3 kcal mol^{-1}, close the values reported by Meier et al. (1982) and Chazotte et al. (1989) describing an L_α phase. The transition temperature (T_m) between the (L_α) phase and the (L_α + L_β) mixed phase is 34 °C for a DMPC/DMPE ratio of 80/20 (Silvius 1986). Below 34 °C, we observe a decrease in the detected amount of electroactive UQ_{10}, as shown in Fig. 2a. Using the same microporous electrode, the experiment was also realized at 44 °C, then at 27 °C and finally at 44 °C again to check the complete reversibility of the transition. The UQ_{10} charge was 9.6×10^{-6} C at 44 °C and 6.8×10^{-6} C at 27 °C. Heating the sample above T_m restores the initial amount of ubiquinone. The decrease in the amount of UQ_{10} can be explained by the formation of domains in the bilayer where ubiquinone molecules are entrapped. Condensation of the lipid bilayer creates L_β domains disconnected from the electrode so that the UQ_{10} in these domains is not detected.

These results show that the presence of a soft aqueous layer minimizes the negative effects of the solid support on the bilayer like the loss of the fluidity of the two-bilayer subfoils. Therefore, the bilayer behaves as a free-standing lipid membrane although it is supported by a polymer cushion and connected to a gold electrode.

Total thickness of the interface

The total thickness of the interface (d_{tot}) is defined as the sum of the thicknesses of the three layers of ADMS (d_{ADMS}), PEG (d_{PEG}) and the bilayer (d_b):

$$d_{\text{tot}} = d_{\text{ADMS}} + d_{\text{PEG}} + d_b \tag{6}$$

In the presence of a cushioned bilayer, the pore diameter is therefore reduced by twice the molecular construction, in other words $2d_{tot}$. As shown in a recent study (Proux-Delrouyre et al. 2002), the thickness of the molecular construction can be measured using an electrochemical method involving forced convection: the rotating disk electrode (RDE). It is applied here to the microporous electrode (Miller and Majda 1986). Briefly, if the thickness of the tethered assembly is significant compared to the pore dimension, the molecular construction will significantly decrease the pore diameter. A Koutecky-Levich analysis of RDE data can be used to measure this decrease expressing the decrease in porosity (P_1) of the oxide (Gough and Leypoldt 1979). The porosity is defined as the relative area of holes calculated from the pore density (P_d) and the pore diameter. Since the pore density of alumina and the porosity are known from independent measurements, we can deduce the average pore diameter for each sample and at each step of the molecular construction.

Three different molecular constructions were tested. PEG chains with molecular weights of 3400 (DSPE-PEG_{3400}), 5000 (PEG_{5000}) and 20000 (PEG_{20000}) were used. The experimental procedure is described elsewhere (Proux-Delrouyre et al. 2002). For each assembly, three measurements of porosity were accomplished, one before fusion of the vesicles, a second after fusion, and a final one after rinsing of the microporous electrode. RDE data were obtained from electrochemical measurements of the diffusion flux of a small, water-soluble, electrochemically-active molecule (ruthenium(III) hexamine), between the bulk solution and the solution confined in the pores of the oxide.

Note that the presence of the PEG chains already grafted does not modify RDE measurements before vesicle fusion. The diffusion of a small molecule is not hindered by the presence of a dilute layer of PEG chains (Levich 1962). Therefore, the experimental value of the porosity represents that of the oxide without the PEG layer. After vesicle fusion, and to prevent the presence of hemi-fused or unfused vesicles, the oxides were extensively rinsed. The measurement performed after this rinsing step assesses the porosity of the oxides decreased by the presence of the polymer-supported bilayer covering the inner surface of the pores. In fact, the presence of the bilayer obstructs the access of the small hydrophilic molecule to the sub-compartment. Before the last measurement, the electrode is dipped in a solution of non- ionic surfactant (octyl glucoside at 5×10^{-2} mol l^{-1}) that solubilizes the bilayer. After a last rinsing, the value of the porosity is the same as the initial one before fusion of the vesicles. Table 1 summarizes the results obtained for the porosity with the three molecular constructions. The thicknesses found for the cushioned lipid bilayers are calculated from:

$$d_{tot} = \sqrt{\frac{P_1}{\pi P_d}} - \sqrt{\frac{P_2}{\pi P_d}} \qquad (7)$$

Table 1 Porosity measurements (by RDE experiments) and thicknesses of the complete molecular structures d_{tot} (ADMS, PEG and bilayer) for the three different polymer cushions

Type of cushion	P_1[a]	P_2[b]	P_3[c]	d_{tot}[d](Å)
DSPE-PEG_{3400}	0.44	0.33	0.45	90 ± 5
PEG_{5000}	0.49	0.34	0.50	110 ± 5
PEG_{20000}	0.50	0.25	0.51	190 ± 10

Conditions for the porosity measurements are described elsewhere (Bourdillon et al. 2002)
[a]Experimental values for the porosity of the oxide before the fusion of the vesicles
[b]Experimental values for the porosity of the oxide after the fusion of the vesicles
[c]Experimental values for the porosity of the oxide after addition of the detergent
[d]Values calculated from Eq. 13

where P_1 and P_2 are the experimental values of the porosity before and after fusion of the vesicles, and P_d is the pore density (3.5×10^{-9} cm^{-2}). The thicknesses found with DSPE-PEG_{3400}, PEG_{5000} and PEG_{20000} were 90, 110, and 190 Å, respectively.

Electron microscopy experiments provide the pore densities of the alumina membranes, while the electrochemistry experiments provide the pore diameters. The thicknesses of the complete molecular architectures (d_{tot}) were deduced from two independent measurements before and after fusion of the vesicles. However, voltammetry experiments alone cannot provide a detailed description of the layers. Therefore, an independent measurement is required to determine the thickness of the polymer cushion (d_{PEG}) and the bilayer thickness (d_b). Among other parameters, the neutron scattering experiments provide the thicknesses of the polymer-cushioned bilayers. Therefore, it is straightforward to determine the thicknesses of the polymer cushions by subtracting the bilayer thicknesses obtained from SANS from the total thicknesses of the interfaces as measured by cyclic voltametry (CV).

Lipid bilayer thickness

According to Eq. 3, if the contrast is such that the alumina is not matched to the water, $I(q)$ is the sum of two terms, one originating from the porous support, the other from the lipid bilayer. The Porod term can be easily suppressed by matching the scattering length density of the solvent to that of alumina. However, using this contrast, there is no more trace of the specific area of the solid support (the Porod term in Eqs. 1, 2 and 3) and it would be nonsense to fit parameters such as the bilayer scattering length density and its specific area at the same time, since these two parameters appear as a product ($\Sigma\ \Delta\ \rho$) in Eqs. 2 and 3. Working at non-zero contrast between the alumina and water is the most convenient way to determine Σ, which is the same for the solid support and the bilayer. The incoherent background would be also much higher at the alumina match

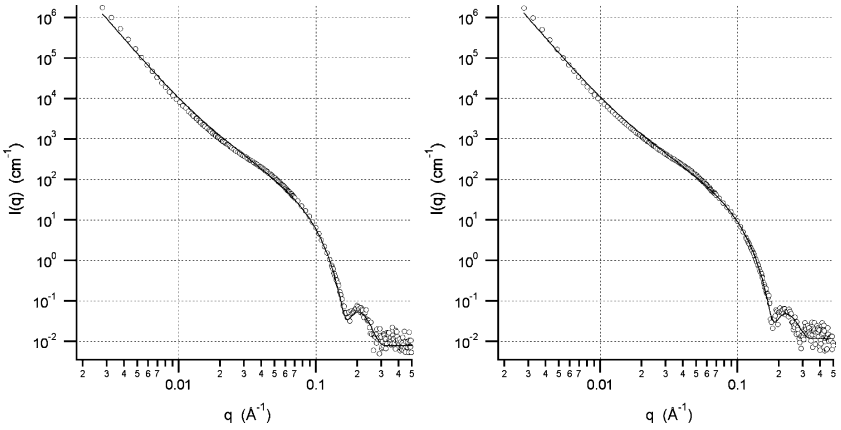

Fig. 4 SANS curves obtained at 30 °C (*left*) and 42 °C (*right*) with the DSPE-PEG3,400-cushioned bilayer confined in a 60 μm-thick alumina membrane. The solvent was pure D_2O. The *solid lines* are the fit to the data according to Eq. 10. The bilayer thicknesses are reported in Table 2 together with those obtained with PEG_{5000} and PEG_{20000} (curves not shown)

point (in D_2O/H_2O 73.1/26.9 v/v) than in pure D_2O. We therefore preferred to work at the best possible contrast (100% D_2O) although this does not correspond to the contrast match point of alumina, a situation where the intensity would result from the bilayer only. Control experiments were performed at the alumina match point in our previous studies. In the fitting procedure several parameters are kept constant to limit the number of adjusted parameters and therefore the number of possible solutions to minimize χ^2. These parameters are the scattering length density of the aqueous phase and that of alumina, which are known from the sample preparation and from a contrast variation experiment, respectively (Marchal et al. 2001a). The roughness of alumina (σ_1) is also kept constant at 2 Å. Like σ_2, it is a very sensitive parameter in the wide-q region (see Marchal et al. (2001a, b) for simulations of the effects of the alumina and bilayer roughnesses.

Figure 4 shows the scattering from a bilayer supported on a DSPE-PEG_{3400} cushion. The lipid bound to the end of the PEG chain is a hydrophobic molecular anchor that inserts into the bilayer when it comes into contact with free vesicles. The curves were measured at 30 and 42 °C, that is below and above the chain melting transition of DMPC/DMPE bilayers (Silvius 1986). The same curves are obtained with PEG_{5000} and PEG_{20000} (not shown). The solid lines are the best fits to the data according to Eq. 3. The scattering length densities of the aqueous phase ($\rho = 6.36\times10^{-6}$ Å^{-2}) and of alumina ($\rho = 4.50\times10^{-6}$ Å^{-2}) are the fixed parameters in the fit, and the specific area is not adjusted between the two temperatures since the sample was the same. The alumina roughness ($\sigma_1 = 2$ Å) is also a constant parameter (Marchal et al. 2001a, b). The fitted thicknesses are 38.0 Å at 30 °C and 34.4 Å at 42 °C. The experiment performed with PEG chains not terminated by a lipid anchor (PEG_{5000} and PEG_{20000}) gave the same bilayer thickness below and above the chain melting transition. So whatever the polymer chain length, and whether lipid anchors are present or not, we find a constant bilayer thickness corresponding to an L_β phase with frozen chains below the chain melting transition and to an L_α above that temperature. Table 2 summarizes the results obtained with the three different types of polymer chains.

Values for the DMPC/DMPE bilayer thicknesses reported in Table 2 show that whatever the kind of polymer—PEG chains of three different molecular weights, with or without lipid anchors—the bilayer binds to the polymer cushion. Its thickness is rigorously the same at 30 °C (38 Å) (below the chain melting transition), the equivalent of a gel (L_β) phase in lyotropic phases, and only slightly different at 42 °C (33 ± 1 Å) above the transition temperature, the equivalent of a fluid (L_α) phase. Differences in the fluid phase are within the uncertainty of the bilayer thickness determination by SANS. It is interesting to note that the presence of the DSPE lipid anchor is not necessary to bind the bilayer to the polymer layer. This confirms the role of PEG chains to promote fusion of the vesicles and to keep the bilayer bound to the cushion without lipid anchor.

Values reported in Table 2 show a bilayer roughness that is rather constant at 7 ± 1 Å whatever the cushion and the temperature, below or above the chain melting transition.

These results are in agreement with the results shown in Sect. 4.1. The thicknesses found correspond to the two phases and confirm the existence of a phase transition, indicating a loosely-bound, free-floating bilayer that reproduces the bulk phase behavior. Note that the RDE technique is not sensitive to thickness changes of a few Angstroms, which can be seen by SANS. The technique is therefore well adapted to studying the phase behavior of single membranes confined in a porous medium, which is not accessible by other sensitive surface techniques.

Table 2 Thicknesses of DMPC/DMPE 80/20 bilayers measured by SANS in the three different molecular assemblies, below and above the chain melting transition temperatures of the bilayers

	T (°C)	d_b (Å)	σ_2 (Å)
DSPE-PEG_{3400}	30	38 ± 1	7 ± 1
	42	34 ± 1	6 ± 1
PEG_{5000}	30	38 ± 1	7 ± 1
	42	33 ± 1	7 ± 1
PEG_{20000}	30	38 ± 1	7 ± 1
	42	34 ± 1	7 ± 1

Table 3 Comparison between calculated and experimental thicknesses of the three molecular constructions at 42 °C. Note the remarkable agreement between the Flory radius of the PEG chains and the value of d_{PEG} calculated from d_b (SANS) and d_{tot} (voltammetry)

Cushion type	N	R_f (Å)	d_{ADMS} (Å)	d_b[a] (Å)	d_{PEG}[b] (Å)	d_{tot}[c] (Å)	$d_{th.}$[d] (Å)
DSPE-PEG_{3400}	77	53	7	34 ± 1	49	90 ± 5	93
PEG_{5000}	114	67	7	33 ± 1	70	110 ± 5	107
PEG_{20000}	455	153	7	34 ± 1	149	190 ± 10	193

[a]Measured by SANS (see Table 2)
[b]Measured by CV–RDE
[c]$d_{PEG} = d_{tot} - d_b - d_{ADMS}$
[d]$d_{th} = d_{ADMS} + R_f + d_b$

Thickness of the polymer layer

Polymer chains in good solvents have a radius given by (Flory 1971):

$$R_f = aN^{3/5} \quad (8)$$

where N is the number of monomers per chain and a is the monomer size. Several values of a are given in the literature for PEG chains (see the recent review by Marsh et al. 2003). Considering the intermediate value of 3.9 Å and using Eq. 6 for PEG chains grafted to a flat solid support (de Gennes 1980; Anne et al. 2002), the theoretical thicknesses of the dilute layers of PEG were found to be 53 Å for PEG_{3400} ($N = 77$), 67 Å for PEG_{5000} ($N = 114$), and 153 Å for PEG_{20000} ($N = 455$). The corresponding thicknesses of the interface (d_{tot}) derived from RDE experiments are 90 Å, 110 Å and 190 Å. Using a thickness of 7 Å for the ADMS layer (Moon 1997), and the bilayer thickness measured by SANS in the fluid phase (34 Å), we obtain the thicknesses of the polymer cushions in the three different molecular assemblies: 49 Å, 69 Å, and 149 Å for PEG_{3400}, PEG_{5000} and PEG_{20000}, respectively. These values are in remarkably good agreement with the theoretical predictions ($d_{th} = d_{ADMS} + R_f + d_b$) given in Table 3. They confirm that the PEG chains confined between the alumina surface and the bilayer are effectively in the mushroom regime and that there is no stretching of the chains due to a high grafting density of PEG chains or to fluctuations of the bilayer that would repel them from the interface. This is not surprising for a lipid mixture that forms rigid bilayers with a high bending rigidity (~20 k_b T for pure DMPC) in the fluid L_α phase.

Conclusion

The microporous electrode offers an original approach to following the construction of tethered or cushioned bilayers and to characterizing their properties. Using grafted PEG chains as polymer cushion for lipid bilayers offers several advantages: (1) it minimizes drawbacks originating from substrate effects like frictional drag between the bilayer and the solid surface, and it restores the fluidity of the two subfoils of the bilayer; (2) it creates a subcompartment with a controlled thickness equal to the Flory radius of the polymer chains in coil configuration; (3) it triggers the fusion of vesicles. All this is in favor of stable, self-assembled, continuous and homogeneous bilayers on large scales. Electrochemical techniques are suitable for following the fluidity of the bilayer through the use of a natural redox probe from the electron transfer chain of biological membranes (UQ_{10}), and for characterizing the thickness of the cushioned bilayer through the use of the modified Koutecky-Levich approach. SANS is the most suitable technique for obtaining structural parameters of a multicomponent molecular assembly confined in such a regular geometry.

Bilayers tethered on such polymer cushions in a microporous electrode are therefore suitable for hosting integral membrane enzymes. By controlling the pool of electrochemically-active compounds, it will be possible to determine the catalytic properties of integral proteins via their co-enzymes.

Therefore, the membrane can be separated from the solid support by a desired distance, depending on the characteristics of the enzyme to be hosted, integral or peripheral, and to the size of its soluble domains.

Controlling the thickness of the aqueous layer separating the membrane from its solid support in the confined geometry provided by porous alumina is important for the confinement and the in situ study of peripheral or integral proteins with soluble parts of variable size. The fact that the thickness of the polymer cushion is in excellent agreement with the Flory radius of the grafted chains is an important result from a theoretical point of view. Density profiles of grafted chains, and therefore the extension of such profiles, cannot be assessed in the case of highly dilute layers (low grafting density). This means that the methodology used here can be applied to the determination of the extension of density profiles in the case of chains grafted to solid interfaces. Until now, this has only been possible using neutron reflectivity on flat solid surfaces or at liquid interfaces and only in the case of chains in the brush regime. In the case of a soft bilayer, the geometry used here is also adapted to the study of fluctuations of a single bilayer smoothly bound to a polymer cushion. The role of the lipid anchor might be important in the case of a fluctuating membrane and should affect the unbinding transition of the bilayer in the absence of lipid anchor.

Acknowledgments This study was made possible thanks to the late Professor J. Moiroux who initiated this work. The authors are grateful to the Institut Laue-Langevin for the allocation of beam time on D16 and D22. DM is grateful to Michel DRUET for the development of the potentiostat.

References

Andrieux CP, Savéant JM (1970) Electrodimerization. I. One electron irreversible dimerization. Diagnostic criteria and rate determination procedures for voltammetric studies. J Electroanal Chem 26:147–186

Anne A, Demaille C, Moiroux J (2002) Terminal attachment of polyethylene glycol (PEG) chains to a gold electrode surface. Cyclic voltammetry applied to the quantitative characterization of the flexibility of the attached PEG chains and of their penetration by mobile PEG chains. Macromolecules 35(14):5578–5586

Bunjes N, Schmidt EK, Jonczyk A, Rippmann F, Beyer D, Ringsdorf H, Graber P, Knoll W, Naumann R (1997) Thiopeptide-supported lipid layers on solid substrates. Langmuir 13(23):6188–6194

Charitat T, Bellet-Amalric E, Fragneto G, Graner F (1999) Adsorbed and free lipid bilayers at the solid–liquid interface. Eur Phys J B 8:583–593

Chazotte B, Hackenbrock CR (1989) Lateral diffusion as a rate-limiting step in ubiquinone-mediated mitochondrial electron transport. J Biol Chem 264:4978–4985

Chazotte B, Wu ES, Hackenbrock CR (1991) The mobility of a fluorescent ubiquinone in model lipid membranes - relevance to mitochondrial electron transport. Biochim Biophys Acta 1058:400–409

Flory P (1971) Principles of polymer chemistry. Cornell University Press, Ithaca, NY

Fournet G (1951) Bull Soc Fr Min Cris 74:37–172

de Gennes PG (1980) Conformations of polymers attached to an interface. Macromolecules 13:1069–1075

Gough DA, Leypoldt JK (1979) Membrane-covered, rotated disk electrode. Anal Chem 51:439–447

Heyse S, Ernst OP, Dienes Z, Hofmann KP, Vogel H (1998) Incorporation of rhodopsin in laterally structured supported membranes: observation of transducin activation with spatially and time-resolved surface plasmon resonance. Biochemistry 37:507–522

Knoll W, Frank CW, Heibel C, Naumann R, Offenhäusser A, Rühe J, Schmidt EK, Shen WW, Sinner A (2000) Functional tethered lipid bilayers. Rev Mol Biotechnol 74:137–158

Lang H, Duschl C, Vogel H (1994) A new class of thiolipids for the attachment of lipid bilayers on gold surfaces. Langmuir 10(1):197–210

Levich VG (1962) Physicochemical hydrodynamics. Prentice-Hall, Englewood Cliffs, NJ

Lipowsky R, Sackmann E (eds) (1996) Elsevier, Amsterdam, pp 903–957

Marchal D, Demé B (2003) Small-angle neutron scattering by porous alumina membranes made of aligned cylindrical channels. J Appl Crystallogr 36:713–717

Marchal D, Boireau W, Laval J-M, Moiroux J, Bourdillon C (1998) Electrochemical measurement of lateral diffusion coefficients of ubiquinones and plastoquinones of various isoprenoid chain lengths incorporated in model bilayers. Biophys J 74:1937–1948

Marchal D, Bourdillon C, Demé B (2001a) Small-angle neutron scattering by highly oriented hybrid bilayer membranes confined in anisotropic porous alumina. Langmuir 17:8313–8320

Marchal D, Pantigny J, Laval J-M, Moiroux J, Bourdillon C (2001b) Rate constants in two dimensions of electron transfer between pyruvate oxidase, a membrane enzyme, and ubiquinone (coenzyme Q8), its water-insoluble electron carrier. Biochemistry 40:1248–1256

Meier P, Blume A, Ohmes E, Neugebauer FA, Kothe G (1982) Structure and dynamics of phospholipid membranes: an electron spin resonance study employing biradical probes. Biochemistry 21:526–534

Miller CJ, Majda M (1985) Microporous aluminium oxide films at electrodes.J Am Chem Soc 107:1419–1420

Miller CJ, Majda M (1986) Microporous aluminiun oxide films at electrodes. Part II - Studies of electron transport in the Al2O3 matrix derivated by adsorbtion of poly(4-vinylpyridine). J Electroanal Chem 207:49–72

Moon JH, Kim JH, Kim K-J, Kang T-H, Kim B, Kim C-H, Hahn JH, Park JW (1997) Absolute surface density of the amine group of the aminosilylated thin layers: ultraviolet-visible spectroscopy, second harmonic generation, and synchrotron-radiation photoelectron spectroscopy study. Langmuir 13:4305–4310

Naumann CA, Prucker O, Lehmann T, Ruhe J, Knoll W, Frank CW (2002) The polymer-supported phospholipid bilayer: tethering as a new approach to substrate-membrane stabilization. Biomacromolecules 3:27–35

Oster G, Riley DP (1952) Acta Crystallogr 5:272–276

Plant AL (1999) Supported hybrid bilayer membranes as rugged cell membrane mimics. Langmuir 15:5128–5135

Porod G (1951) Kolloid Zeitschrift 124:83–114

Proux-Delrouyre V, Laval J-M, Bourdillon C (2001) Formation of streptavidin-supported lipid bilayers on porous anodic alumina: electrochemical monitoring of triggered vesicle fusion. J Am Chem Soc 123:9176–9177

Proux-Delrouyre V, Elie C, Laval J-M, Moiroux J, Bourdillon C (2002) Formation of tethered and streptavidin-supported lipid bilayers on a microporous electrode for the reconstitution of membranes of large surface area. Langmuir 18:3263–3272

Rädler U, Mack J, Persike N, Jung G, Tampe R (2000) Design of supported membranes tethered via metal-affinity ligand-receptor pairs. Biophys J 79:3144–3152

Rajarathnam K, Hochman J, Schindler M, Ferguson-Miller S (1989) Synthesis, location and lateral mobility of fluorescently labeled ubiquinone 10 in mitochondrial and artificial membranes. Biochemistry 28:3168–3176

Rand RP, Parsegian VA (1989) Hydration forces between phospholipid bilayers. Biochim Biophys Acta 988:351–376

Sackmann E (1996) Supported membranes: scientific and pratical applications. Science 271:43–48

Saffman PG, Delbrück M (1975) Browniam motion in biological membranes. Proc Natl Acad Sci USA 72:3111–3113

Schmitt J, Danner B, Bayerl TM (2001) Polymer cushions in supported phospholipid bilayers reduce significantly the frictional drag between bilayer and solid surface. Langmuir 17:244–246

Seitz M, Wong JY,Park CK, Alcantar NA, Israelachvili JJN (1998) Formation of tethered supported bilayers via membrane-inserting reactive lipids. Thin Solid Films 327–329:767–771

Silvius JR (1986) Solid- and liquid-phase equilibria in phosphatidylcholine/phosphatidylethanolamine mixtures. A calorimetric study. Biochim Biophys Acta 857:217–228

Spinke J, Yang J, Wolf H, Liley M, Ringsdorf H, Knoll W (1992) Polymer-supported bilayer on a solid substrate. Biophys J 63:1667–1671

Wagner ML, Tamm LK (2000) Tethered polymer-supported planar lipid bilayers for reconstitution of integral membrane proteins: silane-polyethyleneglycol-lipid as a cushion and covalent linker. Biophys J 79:1400–1414